

Temperature-dependent frequency shifts and broadening of phonon linewidths in lead

This article has been downloaded from IOPscience. Please scroll down to see the full text article.

1991 J. Phys.: Condens. Matter 3 6249

(<http://iopscience.iop.org/0953-8984/3/33/004>)

View [the table of contents for this issue](#), or go to the [journal homepage](#) for more

Download details:

IP Address: 171.66.16.147

The article was downloaded on 11/05/2010 at 12:27

Please note that [terms and conditions apply](#).

Temperature-dependent frequency shifts and broadening of phonon linewidths in lead

Marco Zoli†

Institut für Theoretische Physik, Freie Universität Berlin, Arnimallee 14, 1000 Berlin 33, Federal Republic of Germany

Received 13 February 1991

Abstract. A study of the anharmonic lineshifts and linewidths of phonon modes in lead is presented. The interatomic potential is modelled according to a force constant scheme which includes many-body effects both in the harmonic and anharmonic parts. An enhanced damping of the (0,8,0,0) longitudinal mode is predicted and an explanation for this anomalous behaviour is provided. The results are discussed in connection with the available experimental data.

1. Introduction

The first observations of microscopic anharmonic effects in metals were carried out on lead [1] and aluminum [2]. The temperature-dependent energy broadening of the inelastically scattered neutron groups was interpreted as arising from the lifetimes of the phonons via the uncertainty principle. Since then, some experimental [3–8] and theoretical [9–11] work has been done in order to quantify the effects of the anharmonic interactions on the phonon linewidths and lineshifts in metals. However, because of the difficulty of these measurements the experimental data are affected by errors of 20–25% whereas refined calculations are constrained by long computing times. In some previous papers, theoretical investigations of the phonon self-energy associated with one-phonon scattering processes in noble metals [12, 13], aluminum [12, 14] and palladium [15] have been presented. In particular, it has been shown that:

(i) the room temperature anharmonic effects can be well described in second-order perturbation theory;

(ii) the phonon–phonon scattering theory accounts for the trends observed by the experimentalists in Cu, Al and Pd. Although the Feynmann diagrams which we use to evaluate the phonon self-energy do not contain electron–phonon vertex processes, these contributions are (to some extent) taken into account in our model. In fact, the harmonic and anharmonic interactions have been parametrized according to a force constant scheme which fits experimental phonon frequencies and thermoelastic data. Hence, the theoretical eigenvalues, eigenvectors and interatomic potential also incorporate the many-body effects due to the electronic charge distribution. In other words, we are using dressed phonons and not simply phonons as determined by bare

† On leave from: Institut für Theoretische Physik, Universität Hamburg, Jungiusstrasse 9, 2000 Hamburg 36, Federal Republic of Germany.

ion-ion model potentials. This empirical approach allows one to sample the range of the interatomic forces and to weigh the effects of many-body harmonic and anharmonic interactions.

Among the FCC metals, lead is known to be particularly sensitive to the anharmonic character of the lattice vibrations. Because of the low Debye temperature, $\Theta_D \simeq T_m/7$ where T_m is the melting temperature, the anharmonic effects are visible in a large range of temperatures. Moreover, the comparatively high superconducting transition temperature (7.2 K) indicates that the electron-phonon coupling plays a relevant role in lead. It should also be added that the superconducting transition has negligible influence on the phonon spectrum [16]. In this paper, I present calculations of phonon linewidths and lineshifts in lead along the high symmetry directions of the three-dimensional Brillouin zone (3DBZ).

2. The model

The harmonic part of the interatomic potential contains long range two-body forces and three-body angular forces. The harmonic force constants are defined as follows:

$$\begin{aligned}\alpha_i &= \frac{\phi'(r_i)}{r_i} \\ \beta_i &= \phi''(r_i) \\ \delta_i &= \frac{1}{3a^2} W''(\cos \theta_i^{JKL})\end{aligned}\quad (1)$$

where i labels the neighbour shell; $\phi(r_i)$ is the pairwise potential; $W(\cos \theta^{JKL})$ is the three-body potential and JKL labels the tern of atoms. a is the lattice constant. The parameters in equations (1) are determined by a least-squares fit to the observed phonon frequencies (at 80 K) along the high symmetry directions of the 3DBZ [4]. The experimental second-order elastic constants are also taken into account in the fitting procedure. The range of the potential has to be considerably long to account for the strong Kohn anomalies in the dispersion curves [17]. Two-body forces are therefore extended up to the tenth-neighbour shell and three-body forces, in the last of equations (1), are chosen such that:

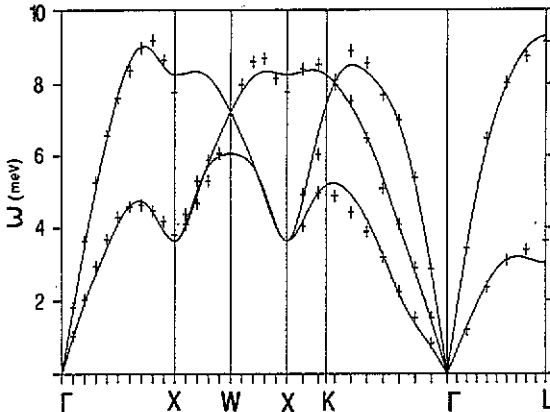
- (i) J and L are nearest neighbours of K;
- (ii) J and L are up to second-neighbours of each other.

In table 1, the harmonic force constants values are reported. In figure 1, the theoretical dispersion relations are shown together with the experimental data. The drop in frequency at the zone boundary observed along the $[\xi, 0, 0]$ direction (and ascribed to a very marked Kohn anomaly [17]) are reproduced by our model. Further extension of the interaction range does not improve the quality of the fitting.

In [13], the anharmonic force constants have been fitted to the experimentally known higher order elastic constants (HOEC) by applying the method of homogeneous deformations. Such an approach does not hold for Pb since the HOEC have not been measured for this metal. Alternatively, the third-order derivatives of the potential are determined by fitting the experimental linear coefficient of thermal expansion at three selected temperatures ($T = 100, 300$ and 500 K) and the room temperature

Table 1. Harmonic and anharmonic force constants values for Pb. The units are 10^{12} dyn cm^{-2} . a is the lattice constant.

$(\beta_1 - \alpha_1)/a$	$(\beta_2 - \alpha_2)/a$	$(\beta_3 - \alpha_3)/a$	$(\beta_4 - \alpha_4)/a$	$(\beta_5 - \alpha_5)/a$
0.265987	0.015388	0.003319	0.026561	-0.009771
$(\beta_6 - \alpha_6)/a$	$(\beta_7 - \alpha_7)/a$	$(\beta_8 - \alpha_8)/a$	$(\beta_9 - \alpha_9)/a$	$(\beta_{10} - \alpha_{10})/a$
0.012361	0.000702	0.018796	0.001718	-0.005115
δ_1/a	δ_2/a	Y_1/a	Y_2/a	Y_3/a
-0.017199	0.005447	-3.4	0.2	-0.1
Z_1/a	Q_1/a	Q_2/a	Q_3/a	—
0.3	19.5	-1.8	0.4	—

**Figure 1.** Phonon dispersion relations in Pb, along the symmetry directions of the Brillouin zone. The pluses are the 80 K experimental values [4].

thermodynamic Grüneisen parameter. The range of the cubic two-body potential has been extended to the third-neighbour shell ($Y_i = r_i \phi''(r_i)$ $i = 1, 2, 3$) and cubic nearest-neighbour angular forces ($Z_1 = (1/3a^2)W''''(\cos \theta^{JKL})$) have been also taken into account. The values of the cubic force constants are reported in table 1. Z_1 plays an essential role in stabilizing the numerical value of the leading force constant Y_1 . This is also indicative of the relevance of many-body effects in the anharmonic tail of the interatomic potential in Pb. The fourth-order derivatives of the two-body potential have been fitted to the experimental constant pressure specific heat at $T = 100, 300$ and 500 K. The values obtained for the force constants $Q_i = r_i^2 \phi''''(r_i)$ $i = 1, 2, 3$, are also listed in table 1.

3. Results and discussion

Due to anharmonicity the frequencies $\omega(\mathbf{q}j)$ of phonons, with wavevector \mathbf{q} and mode index j , are volume- and temperature-dependent. To the lowest order in perturbation theory the harmonic frequencies ω_0 shift to

$$\omega(\mathbf{q}j) = \omega_0(\mathbf{q}j) + \Delta_T(\mathbf{q}j) \quad (2)$$

with

$$\Delta_T(\mathbf{q}j) = \Delta^{(0)}(\mathbf{q}j) + \Delta^{(3)}(\mathbf{q}j) + \Delta^{(4)}(\mathbf{q}j). \quad (3)$$

The shift $\Delta^{(0)}$, which accounts for the dilation effects, is given by

$$\Delta^{(0)}(\mathbf{q}j) = -3\alpha(T)T\gamma(\mathbf{q}j)\omega_0(\mathbf{q}j) \quad (4)$$

where $\alpha(T)$ is the linear coefficient of thermal expansion and $\gamma(\mathbf{q}j)$ is the mode Grüneisen parameter. Both $\alpha(T)$ and $\gamma(\mathbf{q}j)$ are related to the third-order derivatives of the interatomic potential [13]. Hence, the volume-dependent shift $\Delta^{(0)}$ is determined by the very cubic term of the anharmonic Hamiltonian. The terms $\Delta^{(4)}$ and $\Delta^{(3)}$ are the lowest order contributions to the real part of the phonon self-energy and depend on the Fourier transforms of the fourth- and third-order force constant tensors, respectively. They are evaluated at constant volume and their temperature dependence is displayed through the Bose-Einstein statistical factors. Numerical evaluation of $\Delta^{(4)}$ and $\Delta^{(3)}$ requires summations over the wavevectors in the 3DBZ [13]. Because of the many irregularities in the dispersion relations of Pb, particular care has to be taken in the computation of $\Delta^{(3)}$ which contains the principal values of linear combinations of three phonon frequencies. The principal value has been represented by

$$PP\left(\frac{1}{x}\right) = \lim_{\epsilon \rightarrow 0} \frac{x}{x^2 + \epsilon^2} \quad (5)$$

with $\epsilon = 0.5$ meV. Numerical convergence in the second decimal figure of $\Delta^{(3)}$ is achieved by using 49462 points in the first 3DBZ. I have computed $\Delta^{(0)}$, $\Delta^{(4)}$ and $\Delta^{(3)}$ along the three main symmetry directions at 5, 80 and 290 K. The dilation term and the fourth-order contribution are generally small and tend to cancel each other whereas $\Delta^{(3)}$ essentially determines the total shift of the phonon frequencies.

Table 2. Room temperature line shifts of phonons in Pb with respect to 5 K. The shifts are in meV. The wavevectors are in units of $2\pi/a$. Δ_T is defined in equation (2). The experimental data are taken from [6].

\mathbf{q}	Δ_T^a	Δ_{exp}^a	Δ_T^b	Δ_{exp}^b
(0.1 0.0 0.0)	-0.65	-0.28	-0.61	-0.26
(0.3 0.0 0.0)	-1.61	-0.75	-1.02	-0.47
(0.5 0.0 0.0)	-1.23	-0.59	-0.75	-0.42
(0.7 0.0 0.0)	-0.34	-0.16	-0.51	-0.24
(0.9 0.0 0.0)	+0.79	+0.38	+0.82	+0.28
(0.1 0.1 0.1)	-0.69	-0.33	-0.41	-0.21
(0.2 0.2 0.2)	-0.82	-0.38	-0.26	-0.12
(0.3 0.3 0.3)	-0.61	-0.31	-0.74	-0.34
(0.4 0.4 0.4)	-0.55	-0.26	-0.72	-0.33
(0.1 0.1 0.0)	-0.62	-0.31	-0.33	—
(0.3 0.3 0.0)	-1.11	-0.47	-0.78	—
(0.5 0.5 0.0)	-1.62	-0.79	-1.01	—
(0.7 0.7 0.0)	-1.51	-0.73	-0.69	—

^a Longitudinal phonons.

^b Transverse phonons; along the $[\xi\xi 0]$ direction, the data refer to the T_1 branch.

In table 2, the calculated total shifts Δ_T at 290 K are reported for both longitudinal and transverse phonons. To allow a comparison with the available experimental data

[6], the Δ_T values at 5 K have been subtracted from the room temperature values. The agreement between theory and experiment is poor, nonetheless the positive shift observed at large momentum transfers along the $[\xi, 0, 0]$ direction is reproduced by the calculation; at the zone boundary, the anharmonic vibrations stabilize the anomalous drop of the longitudinal and transverse modes. By increasing temperatures the energies of these modes shift upwards and the phonon spectrum tends to flatten. In this view, the irregularities in the dispersion relations of Pb are more visible at low temperatures, say below 100 K, where the long range interatomic forces dominate the dynamics. At higher temperatures, the anharmonic lattice vibrations acquire importance and the shorter range interactions influence the phonon spectrum.

In table 3, the total shifts at 80 K are listed with respect to 5 K. Here the theoretical shifts are larger, in absolute value, than the experimental data. For some low momentum modes, i.e. the (0.3, 0, 0) longitudinal and transverse, the (0.2, 0.2, 0.2) longitudinal and the (0.3, 0.3, 0) transverse, the energy shifts already seem to be appreciable at 5 K. This would be indicative of strong coupling between electrons and some long wavelengths lattice vibrations.

Table 3. Line shifts of phonons in Pb, at 80 K with respect to 5 K. The symbols are defined in table 2.

q	Δ_T^a	Δ_{exp}^a	Δ_T^b	Δ_{exp}^b
(0.1 0.0 0.0)	-0.23	-0.12	-0.20	-0.07
(0.3 0.0 0.0)	-0.63	-0.26	-0.32	-0.15
(0.5 0.0 0.0)	-0.41	-0.19	-0.24	-0.09
(0.7 0.0 0.0)	-0.11	0.0	-0.16	0.0
(0.9 0.0 0.0)	+0.26	+0.19	+0.27	+0.16
(0.1 0.1 0.1)	-0.23	-0.12	-0.14	0.0
(0.2 0.2 0.2)	-0.29	-0.13	-0.08	+0.08
(0.3 0.3 0.3)	-0.21	-0.09	-0.24	-0.09
(0.4 0.4 0.4)	-0.19	-0.07	-0.23	-0.10
(0.1 0.1 0.0)	-0.21	-0.12	-0.12	—
(0.3 0.3 0.0)	-0.34	-0.09	-0.26	—
(0.5 0.5 0.0)	-0.53	-0.16	-0.36	—
(0.7 0.7 0.0)	-0.48	-0.30	-0.31	—

The broadening of the phonon lines is given in second-order perturbation theory by

$$\Gamma(qj) = \frac{18\pi}{\hbar^2} \sum_{q_1, q_2} \sum_{j_1, j_2} |V^{(3)}(-q, j; q_1, j_1; q_2, j_2)|^2 \times \{ (n_1 + n_2 + 1)[\delta(\omega_0(qj) - \omega_0(1) - \omega_0(2)) - \delta(\omega_0(qj) + \omega_0(1) + \omega_0(2))] + (n_1 - n_2)[\delta(\omega_0(qj) + \omega_0(1) - \omega_0(2)) - \delta(\omega_0(qj) - \omega_0(1) + \omega_0(2))] \} \quad (6)$$

where $V^{(3)}$ is the Fourier transform of the third-order force constants tensor and $\omega_0(i) \equiv \omega_0(q_i, j_i)$ and $n_i \equiv n(\omega_0(i))$ are the Bose-Einstein statistical factors. The double sums over the Brillouin zones are reduced to a sum over q_1 because of

translational invariance. Numerical convergence in the second decimal figure is achieved by using around 10 000 points in the first BZ. The method of handling the δ -functions is described in [12]. In table 4, the calculated room temperature linewidths are reported. The discrepancies between theory and experiment are relevant along all the symmetry directions and the computed values are everywhere larger than those measured by Furrer and Halg [6]. In particular, I predict an enhanced damping for the (0.8, 0.0, 0.0) longitudinal mode mainly due to umklapp scattering processes which involve two transverse modes. The value of this phonon width is in fair agreement with that observed by Stedman *et al* [18] at 300 K ($2\Gamma = 1.7$ meV). At some points in q_1 space, the anharmonic coupling $V^{(3)}$ in the three-phonon vertex is strong and the decay process, longitudinal \rightarrow transverse + transverse is favoured. Such points together with the frequencies of the corresponding transverse phonons are given in table 5. A high density of final states should be expected for this scattering process.

Table 4. Room temperature linewidths for Pb, in meV. The experimental data are taken from [6].

q	$2\Gamma^a$	$2\Gamma_{\text{exp}}^a$	$2\Gamma^b$	$2\Gamma_{\text{exp}}^b$
(0.1 0.0 0.0)	0.11	0.03	0.18	0.02
(0.3 0.0 0.0)	0.25	0.10	0.34	0.04
(0.5 0.0 0.0)	0.81	0.26	1.14	0.09
(0.7 0.0 0.0)	1.25	0.20	0.94	0.15
(0.8 0.0 0.0)	1.84	0.22	0.93	0.16
(0.9 0.0 0.0)	1.52	0.27	0.75	0.16
(1.0 0.0 0.0)	1.28	0.47	0.50	0.14
(0.1 0.1 0.1)	0.36	0.05	0.19	0.02
(0.2 0.2 0.2)	0.24	0.18	0.37	0.04
(0.3 0.3 0.3)	0.78	0.14	0.46	0.05
(0.4 0.4 0.4)	1.05	0.22	0.57	0.07
(0.1 0.1 0.0)	0.16	0.04	0.14	—
(0.3 0.3 0.0)	0.46	0.19	0.39	—
(0.5 0.5 0.0)	0.87	0.35	0.79	—
(0.7 0.7 0.0)	1.38	0.41	0.75	—

^a Longitudinal phonons.

^b Transverse phonons; along the $[\xi\xi 0]$ direction, the data refer to the T_1 branch.

At 80 K the linewidths are about one-third of the room temperature values, consistently with the reduction of the experimental data. The Bose-Einstein distributions govern the linear temperature dependence of the linewidths in the range 80–290 K. I have also calculated equation (6) at 425 K to allow a comparison with the first measurements of phonon linewidths which were carried out by Brockhouse *et al* [1]. For the (0.8, 0, 0) longitudinal mode the theory yields a linewidth of 2.4 meV whereas the experimental value is 1.95 meV.

In conclusion, the evaluation of the phonon self-energies in lead shows that the lattice dynamics in this metal is strongly influenced by anharmonic interactions. The frequencies of the phonon spectrum are always lower than 10 meV so that the computed lineshifts Δ_T and linewidths 2Γ are relatively much larger in lead than in the other FCC metals. For the (0.8, 0, 0) longitudinal mode the ratio $2\Gamma/\omega_0$ is $\simeq 0.2$ at room temperature and, at these values, the applicability of a perturbative approach

Table 5. Anomalous umklapp scattering processes for the (0.8, 0.0, 0.0) longitudinal mode in Pb. In the q_1 space points listed in the first column, the three-phonon vertex coupling is strong. The wavevectors are in units of $2\pi/a$. $\omega_0(q_1j_1)$ and $\omega_0(q_2j_2)$ are the energies (in meV) of the transverse phonons which originate from the decay of the longitudinal mode. $q_2 = q - q_1 + G$, where G is a reciprocal lattice vector.

q_1	$\omega_0(q_1j_1)$	$\omega_0(q_2j_2)$
(0.0 -0.744 \pm 0.133)	4.73	3.91
(\pm 0.033 -0.755 \pm 0.133)	4.80	3.84
(\pm 0.033 -0.445 \pm 0.133)	3.84	4.80
(\pm 0.1 -0.957 \pm 0.3)	6.52	2.12
(\pm 0.1 -0.507 \pm 0.066)	4.0	4.64
(\pm 0.1 -0.692 \pm 0.066)	4.64	4.0
(\pm 0.133 -0.637 \pm 0.633)	4.37	4.27
(\pm 0.133 -0.562 \pm 0.633)	4.27	4.37
(\pm 0.2 -0.208 \pm 0.466)	3.44	5.20
(\pm 0.2 -0.167 \pm 0.466)	3.45	5.19
(\pm 0.233 -0.376 \pm 0.433)	3.91	4.73
(\pm 0.233 -0.483 \pm 0.7)	4.30	4.34
(\pm 0.266 -0.681 \pm 0.466)	4.10	4.54
(\pm 0.266 -0.518 \pm 0.466)	4.54	4.10
(\pm 0.533 -0.032 \pm 0.8)	5.19	3.45
(\pm 0.533 +0.008 \pm 0.8)	5.20	3.44
(\pm 0.766 +0.283 \pm 0.3)	4.34	4.30

may be doubtful. In view of the fact that the available experimental data [6] and [18] are in conflict, it is my hope that new experimental research will be devoted to establishing the possible existence and relevance of enhanced dampings of phonon modes in lead.

Acknowledgments

I wish to thank Professor A Furrer for correspondence on the subject matter of this paper. I am grateful to S Russ and T Wölkhausen for their kind collaboration during my staying in Hamburg. Numerical calculation were carried out at the Rechenzentrum, University of Hamburg, Germany.

References

- [1] Brockhouse B N, Caglioti G, Sakamoto M, Sinclair R N and Woods A D B 1960 *Bull. Am. Phys. Soc.* 5 39
- [2] Larsson K E, Dahlborg U and Holmryd S 1960 *Ark. Fys.* 17 369
- [3] Brockhouse B N, Rao K R and Woods A D B 1961 *Phys. Rev. Lett.* 7 93
- [4] Stedman R and Nilsson G 1966 *Phys. Rev.* 145 492
- [5] Buyers W J L and Cowley R A 1969 *Phys. Rev.* 180 755
- [6] Furrer A and Hälgl W 1970 *Phys. Status Solidi* 42 821
- [7] Müller A P 1975 *Can. J. Phys.* 53 2491
- [8] Larose A and Brockhouse B N 1976 *Can. J. Phys.* 54 1990
- [9] Maradudin A A and Fein A E 1962 *Phys. Rev.* 128 2589
- [10] Koehler T R, Gillis M S and Wallace D C 1970 *Phys. Rev. B* 1 4521
- [11] Pinski F J and Butler W H 1979 *Phys. Rev. B* 19 6010

- [12] Zoli M, Santoro G, Bortolani V, Maradudin A A and Wallis R F 1990 *Phys. Rev. B* **41** 7507
- [13] Zoli M 1990 *Phys. Rev. B* **41** 7497
- [14] Zoli M 1990 *Phil. Mag. Lett.* **62** 203
- [15] Zoli M 1990 *J. Phys.: Condens. Matter* **2** 8859
- [16] Waldorf D and Alers G A 1962 *J. Appl. Phys.* **33** 3266
- [17] Brockhouse B N, Arase T, Caglioti G, Rao K R and Woods A B B 1962 *Phys. Rev.* **128** 1099
- [18] Stedman R, Almqvist L, Nilsson G and Raunio G 1967 *Phys. Rev.* **162** 545